Inorg. Chem. **2006**, *45*, 7126–7132

$Ba_{11}Cd_8Bi_{14}$: Bismuth Zigzag Chains in a Ternary Alkaline-Earth Transition-Metal Zintl Phase

Sheng-qing Xia and Svilen Bobev*

Department of Chemistry and Biochemistry, University of Delaware, Newark, Delaware 19716

Received April 6, 2006

A new transition-metal-containing Zintl phase, $Ba_{11}Cd_8Bi_{14}$, has been synthesized by a Cd-flux reaction, and its structure has been determined by a single-crystal X-ray diffraction. $Ba_{11}Cd_8Bi_{14}$ crystallizes in the monoclinic space group *C2/m* (No. 12, $Z = 2$) with $a = 28.193(8)$ Å, $b = 4.8932(14)$ Å, $c = 16.823(5)$ Å, and $\beta = 90.836(4)°$, taken at –150 °C (R1 = 0.0407, wR2 = 0.1016). The structure can be described as being built of complex polyanionic $[Cd_8Bi_{14}]^{22-}$ layers running along the *b* axis, which are separated by the Ba^{2+} cations. An interesting feature of these layers is that they are composed of novel centrosymmetric chains of corner- and edge-shared $CdBi_4$ tetrahedra, interconnected through *exo*-Bi–Bi bonds. These bonds connect terminal Bi atoms from adjacent chains in such a way that infinite zigzag chains of bismuth parallel to the same direction are formed. Electronic band structure calculations performed using the TB-LMTO-ASA method show a very small band gap, suggesting a narrow-gap semiconducting or poor metallic behavior for $Ba_{11}Cd_8Bi_{14}$. The crystal orbital Hamilton population (COHP) analysis on the homo- and heteroatomic interactions in this structure is reported as well.

Introduction

The classical Zintl phases are the binary and ternary compounds composed of the less electronegative alkali or alkaline-earth metals and the more electronegative post-transition metalloid elements.[1−5] Their structures can simply be rationalized by assuming a complete valence electron transfer from the electropositive elements to the electronegative components, whereby each element achieves a closed-shell state conforming to the octet rule.[2,3] In the past twenty years, the Zintl formalism has been extended to include a greater number of elements, including the lanthanides and some of the transition metals that commonly have d^0, d^5, and d^{10} configurations.[4−15] Many such compounds with diverse structures and unique magnetic and electronic properties have already been synthesized and studied. For instance, Zintl compounds containing the heavier p-block elements, such as $Ba_4In_8Sb_{16}$,[15] $Yb_{11}GaSb_9$,[6] and $BaGa_2Sb_2$,[7]

* To whom correspondence should be addressed. Phone: (302) 831-8720. Fax: (302) 831−6335. E-mail: sbobev@chem.udel.edu.

(1) (a) Kauzlarich, S. M. In *Chemistry, Structure, and Bonding of Zintl Phases and Ions*; Kauzlarich, S. M., Ed.; VCH Publishers: New York, 1996, p 245. (b) Corbett, J. D. In *Chemistry, Structure, and Bonding of Zintl Phases and Ions*; Kauzlarich, S. M., Ed.; VCH Publishers: New York, 1996, p 139. (c) Eisenmann, B.; Cordier, G. In *Chemistry, Structure, and Bonding of Zintl Phases and Ions*; Kauzlarich, S. M., Ed.; VCH Publishers: New York, 1996, p 61.
(2) Zintl, E. *Angew. Chem.* **1939**, *52*, 1−6.
(3) Nesper, R. *Prog. Solid State Chem.* **1990**, *20*, 1−45.
(4) (a) Eisenmann, B.; Schäfer, H. *Rev. Inorg. Chem.* **1981**, *3*, 29−101. (b) Corbett, J. D. *Angew. Chem., Int. Ed.* **2000**, *39*, 670−681.
(5) Schäfer, H. *Annu. Rev. Mater. Sci.* **1985**, *15*, 1−41.
(6) Bobev, S.; Frisch, V.; Thompson, J. D.; Sarrao, J. L.; Eck, B.; Dronskowski, R.; Kauzlarich, S. M. *J. Solid State Chem.* **2005**, *178*, 1071−1079.
(7) Kim, S.-J.; Kanatzidis, M. G. *Inorg. Chem.* **2001**, *40*, 3781−3785.
(8) Mill, A. M.; Deakin, L.; Mar, A. *Chem. Mater.* **2001**, *13*, 1778−1788.
(9) (a) Lam, R.; Mar A. *Inorg. Chem.* **1996**, *35*, 6959−6936. (b) Deakin, L.; Lam, R.; Marsiglio, F.; Mar, A. *J. Alloys Compd.* **2002**, *388*, 69−72.
(10) (a) Chan, J. Y.; Kauzlarich, S. M.; Klavins, P.; Liu, J.-Z.; Shelton, R. N.; Webb, D. J. *Phys. Rev. B* **2000**, *61*, 459−463. (b) Chan, J. Y.; Kauzlarich, S. M.; Klavins, P.; Shelton, R. N.; Webb, D. J. *Chem. Mater.* **1997**, *9*, 3132−3135. (c) Chan, J. Y.; Kauzlarich, S. M.; Klavins, P.; Shelton, R. N.; Webb, D. J. *Phys. Rev. B* **1998**, *57*, 8103−8106. (d) Kim, H.; Chan, J. Y.; Olmstead, M. M.; Klavins, P.; Webb, D. J.; Kauzlarich, S. M. *Chem. Mater.* **2002**, *14*, 206−216. (e) Sánchez-Portal, D.; Martin, R. M.; Kauzlarich, S. M.; Pickett, W. E. *Phys. Rev. B* **2002**, *65*, 144414. (f) Holm, A. P.; Kauzlarich, S. M.; Morton, S. A.; Waddill, G. D.; Pickett, W. E.; Tobin, J. G. *J. Am. Chem. Soc.* **2002**, *124*, 9894−9898.
(11) (a) Brechetel, E.; Cordier, G.; Schäfer, H. *Z. Naturforsch.* **1979**, *34B*, 1229−1233. (b) Brechetel, E.; Cordier, G.; Schäfer, H. *J. Less-Common Met.* **1981**, *79*, 131−138.
(12) (a) Cordier, G.; Schäfer, H.; Stelter, M. *Z. Anorg. Allg. Chem.* **1984**, *519*, 183−188. (b) Cordier, G.; Schäfer, H.; Stelter, M. *Z. Naturforsch.* **1984**, *39B*, 727−732. (c) Cordier, G.; Czech, E.; Jakowski, M.; Schäfer, H. *Rev. Chim. Miner.* **1981**, *18*, 9−18. (d) Cordier, G.; Stelter, M.; Schäfer, H. *J. Less-Common Met.* **1984**, *98*, 285−290. (e) Cordier, G.; Stelter, M. *Z. Naturforsch.* **1988**, *43*, 463−466.
(13) (a) von Schnering, H.-G.; Kröner, R.; Carrillo-Cabrera, W.; Peters, K.; Nesper, R. *Z. Kristallogr.−New Cryst. Struct.* **1998**, *213*, 665−666. (b) Kim, S.-J.; Hu, S.-Q.; Uher, C.; Hogan, T.; Huang, B.-Q.; Corbett, J. D.; Kanatzidis, M. G. *J. Solid State Chem.* **2000**, *153*, 321−329.

10.1021/ic060583z CCC: $33.50
Published on Web 07/27/2006

are found to be narrow band-gap p-type semiconductors, while the rare-earth gallium antimonides, such as $La_{13}Ga_8Sb_{21}$,[8] $Ba_2Sn_3Sb_6$, and $SrSn_3Sb_4$, are superconducting.[9] In the $E_{14}MnPn_{11}$ family alone (E = Ca, Sr, Ba, Eu, or Yb; Pn = P, As, Sb, or Bi), intriguing ferromagnetism and colossal magnetoresistance have been reported.[10] Recent work in the area also shows a high thermoelectric figure of merit and suggests application of such intermetallic compounds as prospective thermoelectric materials.[15,16]

As part of the ongoing efforts to elucidate the complicated structure−property relationships in various transition-metal-based Zintl phases and related polar intermetallic compounds, we turned our attention to the Ba−Cd−Bi system. The initial focus of this work was to synthesize and characterize the unknown ternary compound $Ba_9Cd_{4+x}Bi_9$, which is isostructural with the recently reported $Yb_9Zn_{4+x}Sb_9$ ($0 < x < 0.5$).[17] These studies were aimed at better understanding the structural complexity along with the possible phase width and their effects on the poorly understood physical properties of these ternary phases. Instead, the reactions of Ba, Cd, and Bi resulted in the discovery of a new material, $Ba_{11}Cd_8Bi_{14}$, with a unique layered polyanionic framework, composed of $[Cd_8Bi_{14}]$ infinite ribbons connected to each other through zigzag chains of Bi. TB-LMTO-ASA calculations suggest $Ba_{11}Cd_8Bi_{14}$ to be a charge-balanced compound (i.e. a Zintl phase) which might exhibit interesting electronic or thermoelectric properties.

Experimental Section

Synthesis. All manipulations were performed inside an argon-filled glovebox or under vacuum. The metals were used as received: Ba (Aldrich, rod, 99+%), Cd (Alfa, shot, 99.999%), and Bi (Alfa, rod, 99.99%). The reaction was carried out by loading the starting materials in a Ba/Cd/Bi ratio of 1:5:1 in an alumina crucible, which was subsequently sealed in an evacuated fused silica jacket. The reaction mixture was heated from room temperature to 700 °C at a rate of 200 °C/h, allowed to homogenize at this temperature for 24 h, and subsequently slowly cooled to 400 °C at a rate of 5 °C/h. Then the ampule was removed from the furnace, quickly inverted and placed into a centrifuge to spin off the excess of molten Cd for about 20−30 s. The reaction vessel was opened in the glovebox, and the product was a mixture of three phases: black, irregularly shaped crystals of the title compound (main product, est. yield > 70%), a few silver, needlelike crystals of $BaCd_{11}$ (minor phase, ca. 10−15%),[18] and small, black platelike crystals of $Ba_2Cd_3Bi_4$ (minor phase, ca. 10−15%).[19] Attempts to produce $Ba_{11}Cd_8Bi_{14}$ from an "on-stoichiometry" reaction in welded Nb tubes failed.

The Cd-flux grown crystals of $Ba_{11}Cd_8Bi_{14}$ are irregularly shaped and black. They are very air- and moisture-sensitive and quickly decompose upon removal from the glovebox, which precludes microprobe analysis. Because of this extreme sensitivity, all attempts to measure the resistance were hampered and could not provide reliable information on the conductivity.

Table 1. Selected Crystal Data and Structure Refinement Parameters for $Ba_{11}Cd_8Bi_{14}$

empirical formula	$Ba_{11}Cd_8Bi_{14}$
fw	5335.66 g/mol
data collection temp	−150 °C
radiation, wavelength (λ)	Mo Kα, 0.71073 Å
cryst syst	monoclinic
space group	*C*2/*m* (No. 12)
unit cell dimensions	a = 28.193(8) Å
	b = 4.893(1) Å
	c = 16.823(5) Å
	β = 90.836(4)°
unit cell volume, Z	2320.5(11) Å^3, 2
density (ρ_{calcd})	7.636 g/cm^3
abs coeff (μ)	655.72 cm^{-1}
final R indices[a] [$I > 2\sigma_{(I)}$]	R1 = 0.0407, wR2 = 0.1016
final R indices[a] [all data]	R1 = 0.0563, wR2 = 0.1080

[a] $R1 = \sum||F_o| - |F_c||/\sum|F_o|$; $wR2 = [\sum[w(F_o^2 - F_c^2)^2]/\sum[w(F_o^2)^2]]^{1/2}$, where $w = 1/[\sigma^2F_o^2 + (0.0519P)^2 + 118.2488P]$, $P = (F_o^2 + 2F_c^2)/3$.

Powder X-ray Diffraction. X-ray powder diffraction patterns were taken at room temperature on a Rigaku MiniFlex powder diffractometer using monochromatized Cu Kα radiation. The data analysis was carried out using the JADE 6.5 software package.[20] Samples were prepared inside the glovebox by grinding crystals of $Ba_{11}Cd_8Bi_{14}$ to a fine powder, placing it in the sample holder, and covering the surface with a thin film of Apiezon grease. This was done to prevent the crystallites from oxidation during the data collection. Because of the low symmetry and fairly large unit cell and the compound's sensitivity and quick decomposition, the powder patterns were with very poor intensity statistics and problematic background. For these reasons, the analysis of the data was not conclusive.

Single-Crystal X-ray Diffraction. A crystal suitable for data collection was selected in a glovebox, cut in Paratone N oil to the desired smaller dimensions (0.06 × 0.04 × 0.02 mm^3), and then mounted on a glass fiber. It was quickly placed on the goniometer of a Bruker SMART CCD-based diffractometer, operated at ca. −150 °C (cooled with liquid nitrogen). The intensity data were collected in batch runs at different ω and ϕ angles. The frame width was 0.4° in ω and θ with a data acquisition time of 20 s/frame. The data collection, data integration, and cell refinement were done using the SMART and SAINT programs,[21] respectively (T_{min}/T_{max} = 0.077/0.270, R_{int} = 0.051). SADABS [22] was used for semiempirical absorption correction based on equivalents. Further details on the data collection and structure refinements are given in Table 1.

The systematic absence of reflections with indexes *hkl*, *hk*0 ($h + k \neq 2n$); *h*0*l*, *h*00 ($h \neq 2n$); and 0*kl*, 0*k*0 ($k \neq 2n$)) confirmed the *C*-centering of the cell and suggested three possible space groups: *C*2 (No. 5), *Cm* (No. 8), and *C*2/*m* (No. 12). The intensity statistics were consistent with a centrosymmetric symmetry, and the structure was solved in *C*2/*m* by direct methods and refined by full matrix least-squares methods on F^2 using SHELX.[23] The initial refinement cycles with isotropic thermal parameters confirmed the validity of the model and converged to an *R* value below 12%.

(14) Mills A. M.; Lam R.; Ferguson M. J.; Deakin L.; Mar A. *Coord. Chem. Rev.* **2002**, *233*−*234*, 207−222.
(15) Kim, S.-J.; Hu, S.; Uher, C.; Kanatzidis, M. G. *Chem. Mater.* **1999**, *11*, 3154−3159.
(16) Chung, D.-Y.; Hogan, T.; Brazis, P.; Rocci-Lane, M.; Kannewurf, C.; Bastea, M.; Uher, C.; Kanatzidis, M. G. *Science* **2000**, *287*, 1024−1027.
(17) Bobev, S.; Thompson, J. D.; Sarrao, J. L.; Olmstead, M. M.; Hope, H.; Kauzlarich, S. M. *Inorg. Chem.* **2004**, *43*, 5044−5052.
(18) Sanderson, M. J.; Baenziger, N. C. *Acta Crystallogr.* **1953**, *6*, 627−631.
(19) Cordier, G.; Woll, P.; Schäfer, H. *J. Less-Common Met.* **1982**, *86*, 129−136.
(20) *JADE*, version 6.5; Materials Data, Inc.: Livermore, CA, 2003.
(21) *SMART* and *SAINT*; Bruker AXS Inc.: Madison, WI, 2002.
(22) Sheldrick, G. M. *SADABS*; University of Göttingen: Göttingen, Germany, 2003.
(23) Sheldrick, G. M. *SHELXTL*; University of Göttingen: Göttingen, Germany, 2001.

Table 2. Atomic Coordinates and Equivalent Isotropic Displacement Parameters (U_{eq})[a] for $Ba_{11}Cd_8Bi_{14}$

atom	Wyckoff position	x	y	z	U_{eq} (Å^2)
Ba1	4*i*	0.3441(1)	0	0.1007(1)	0.013(1)
Ba2	2*b*	0	1/2	0	0.012(1)
Ba3	4*i*	0.3822(1)	0	0.8393(1)	0.013(1)
Ba4	4*i*	0.0088(1)	0	0.3678(1)	0.014(1)
Ba5	4*i*	0.1456(1)	0	0.5336(1)	0.016(1)
Ba6	4*i*	0.2532(1)	0	0.2970(1)	0.020(1)
Cd1	4*i*	0.3715(1)	0	0.6125(1)	0.038(1)
Cd2	4*i*	0.0601(1)	0	0.8414(1)	0.014(1)
Cd3	4*i*	0.2019(1)	0	0.0404(1)	0.014(1)
Cd4	4*i*	0.4052(1)	0	0.3148(1)	0.015(1)
Bi1	4*i*	0.4910(1)	0	0.2099(1)	0.013(1)
Bi2	4*i*	0.4404(1)	0	0.4823(1)	0.018(1)
Bi3	4*i*	0.0936(1)	0	0.0121(1)	0.011(1)
Bi4	4*i*	0.1493(1)	0	0.7381(1)	0.014(1)
Bi5	4*i*	0.1300(1)	0	0.3021(1)	0.017(1)
Bi6	4*i*	0.2580(1)	0	0.8834(1)	0.012(1)
Bi7	4*i*	0.2719(1)	0	0.5407(1)	0.042(1)

[a] U_{eq} is defined as one-third of the trace of the orthogonalized U^{ij} tensor.

During the subsequent structure refinements with anisotropic thermal parameters, however, a problem with the temperature parameters for Cd1 and Bi7 became apparent: their shapes were abnormally elongated in a direction almost parallel to the Cd−Bi bond. Additionally, a peak of relatively significant height, ca. 10 e/Å^3, and less than 1.7 Å away from both Bi7 and Cd1 was left in the difference Fourier map. In the next refinement cycles, both atoms were refined with freed occupation factors, which resulted in marginal improvement of their displacement parameters and occupancies around 90% with large standard deviations. After elaborate refinements, it became clear that these problems were stemming from a small positional disorder. All attempts to solve and refine the structure in lower symmetry (in both *Cm* and *C*2 and even in *P*1) did not provide evidence for the existence of a long-range ordering. Detailed discussion on the disorder and various models involving possible split positions has been provided as Supporting Information.

In the last refinement cycles, the atomic positions were standardized using STRUCTURE TIDY,[24] and all sites were refined with anisotropic displacement parameters. Final positional and equivalent isotropic displacement parameters and important bond distances and angles are listed in Tables 2 and 3, respectively. Further information in the form of CIF has been deposited with Fachinformationzentrum Karlsruhe, 76344 Eggenstein-Leopoldshafen, Germany (fax (49) 7247-808-666; e-mail crysdata@fiz.karlsruhe.de), depository number CSD 416345.

Electronic Structure Calculations. TB-LMTO-ASA calculations were carried out by applying the LMTO-47 package.[25] This program is based on the tight-binding linear-muffin-tin orbital (LMTO) method in the local density (LDA) and atomic sphere (ASA) approximations.[26] Reciprocal space integrations are calculated by the tetrahedron method.[27] The crystal orbital Hamilton population (COHP) method is used for the analysis of bonding interactions,[28] analogous to the crystal orbital overlap population (COOP) method used in the semiempirical Hückel calculations.[29] The Fermi levels in all figures are set to zero, and the COHP diagrams are drawn by reversing their values with respect to the energy scale (i.e., −COHP vs *E*). This is done so that the calculated peak values are negative for antibonding and positive for bonding interactions.

Table 3. Selected Bond Distances in $Ba_{11}Cd_8Bi_{14}$

atom pair		distance (Å)	atom pair		distance (Å)
Bi1−	Cd2 (×2)	2.960(1)	Ba1−	Bi3 (×2)	3.574(1)
	Cd4	3.014(2)		Bi4 (×2)	3.655(1)
Bi2−	Cd1	2.947(3)		Bi6 (×2)	3.789(2)
	Cd4	2.973(2)		Cd2 (×2)	3.763(2)
	Bi2	3.406(2)		Cd3 (×2)	3.636(2)
Bi3−	Cd2	3.010(2)		Cd3	4.120(3)
	Cd3	3.085(2)		Cd4	3.970(3)
Bi4−	Cd4 (×2)	3.017(1)	Ba2−	Bi1 (×2)	3.543(1)
	Cd2	3.079(2)		Bi3 (×4)	3.602(1)
Bi5−	Cd1 (×2)	2.838(2)		Cd2 (×4)	4.013(2)
Bi6−	Cd3 (×2)	2.978(1)	Ba3−	Bi1	3.682(2)
	Cd3	3.098(2)		Bi3 (×2)	3.557(2)
Bi7−	Cd1	3.042(3)		Bi5 (×2)	3.426(2)
	Bi7 (×2)	3.055(2)		Bi6	3.591(2)
Cd1−	Bi5 (×2)	2.838(2)		Cd1	3.823(3)
	Bi2	2.947(3)		Cd3 (×2)	3.981(2)
	Bi7	3.042(3)	Ba4−	Bi1 (×2)	3.642(2)
Cd2−	Bi1 (×2)	2.960(1)		Bi2 (×2)	3.677(2)
	Bi3	3.010(2)		Bi2 (×2)	3.781(2)
	Bi4	3.079(2)		Bi5	3.607(2)
Cd3−	Bi6 (×2)	2.978(1)		Cd2	3.995(3)
	Bi3	3.085(2)		Cd4 (×2)	3.903(2)
	Bi6	3.098(2)	Ba5−	Bi2 (×2)	3.451(2)
Cd4−	Bi2	2.973(2)		Bi4	3.440(2)
	Bi1	3.014(2)		Bi5	3.913(2)
	Bi4 (×2)	3.017(1)		Bi7	3.561(2)
				Bi7 (×2)	3.612(2)
				Cd1 (×2)	3.496(2)
				Cd4 (×2)	3.827(2)
			Ba6−	Bi4 (×2)	3.732(2)
				Bi5	3.476(2)
				Bi6 (×2)	3.906(2)
				Bi7 (×2)	3.742(2)
				Bi7	4.126(3)

Results and Discussion

Synthesis, Structure, and Bonding. $Ba_{11}Cd_8Bi_{14}$ was initially discovered as one of the products of a reaction of Ba, Cd, and Bi carried out in Cd flux. The reaction was intended to produce the hitherto unknown phase $Ba_9Cd_{4+x}Bi_9$, isotypic with $Yb_9Zn_{4+x}Sb_9$ ($0 < x < 0.5$).[17] Subsequent attempts to make the title compound in large yields from an "on-stoichiometry" reaction were unsuccessful: the outcomes of these were inhomogeneous mixtures of Bi, Cd, and another poorly crystalline Ba−Cd−Bi compound with very large cell constants (cell volume ca. 4000 Å^3), which is most likely a new ternary compound (or perhaps a derivative of the title compound). This means that $Ba_{11}Cd_8Bi_{14}$ is either a metastable phase, which grows in the Cd-rich melt or it forms by a peritectic reaction. Thus, after the tetragonal $BaCdBi_2$[11b] and the orthorhombic $Ba_2Cd_3Bi_4$,[19] $Ba_{11}Cd_8Bi_{14}$ is only the third structurally characterized phase involving Ba, Cd, and Bi. Evidently, in this and in other systems based on the electropositive metals from the left-hand side of the periodic table, early p-block or late transition metals and the pnico-

(24) (a) Parthe, E.; Gelato, L. M. *Acta Crystallogr.* **1984**, *A40*, 169−183. (b) Gelato, L. M.; Parthe, E. *J. Appl. Crystallogr.* **1987**, *20*, 139−143.
(25) Jepsen, O.; Andersen, O. K. *TB-LMTO-ASA Program*, version 4.7; Max-Planck-Institut Für Festkörperforschung: Stuttgart, Germany, 1998.
(26) Andersen, O. K.; Jepsen, O. *Phys. Rev. Lett.* **1984**, *53*, 2571−2574.
(27) Blochl, P.; Jepsen, O.; Andersen, O. K. *Phys. Rev. B.* **1994**, *34*, 16223−16233.
(28) Dronskowski, R.; Blochl, P. *J. Phys. Chem.* **1993**, *97*, 8617−8624.
(29) Hughbanks, T.; Hoffmann, R. *J. Am. Chem. Soc.* **1983**, *105*, 3528−3537.

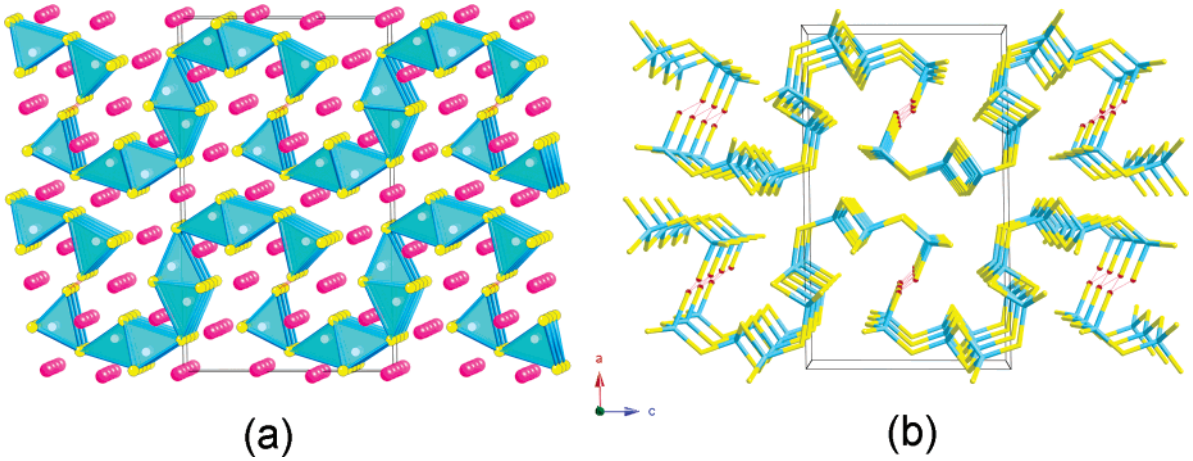

Figure 1. (a) Polyhedral view of the structure of $Ba_{11}Cd_8Bi_{14}$, viewed down the *b* axis. Ba atoms are drawn as magenta spheres; the Bi atoms are drawn as yellow spheres, and the Cd atoms are shown with small light spheres inside the translucent light blue tetrahedra, respectively. (b) A perspective skeletal view of the structure, where the topology of the polyanionic network is emphasized, while the Ba cations are omitted for clarity. The unit cell is outlined in both projections.

gens, the Bi-rich phases are rare and not as common as their As and Sb counterparts.[6−9,12−15] This general observation may indicate that the corresponding "phase-space" is poorly mapped and that more systematic syntheses can reveal an unexpected wealth of new bonding patterns and properties.

$Ba_{11}Cd_8Bi_{14}$ crystallizes in a new type with monoclinic symmetry (Table 1). There are 7 unique bismuth sites, 4 unique cadmium sites, and 6 unique barium sites in its structure, all in special positions (Table 2). The implication of that is easily seen in Figure 1: the structure is fairly complicated, especially at first sight. Similarly, complex structures with the same *C*-centered monoclinic group (*C*2/*m*) are known, for example, the recently reported $Sr_{11}Cd_6Sb_{12}$,[30] $Eu_{10}Mn_6Sb_{13}$,[31] and $Ca_{21}Mn_4Sb_{18}$.[32] These structures and the structure of $Ba_{11}Cd_8Bi_{14}$, however, are not similar.

Schematic representations of the structure projected down the unique *b* axis are given in both polyhedral (Figure 1a) and skeletal mode (Figure 1b). The structure consists of cadmium-centered tetrahedra of bismuth, which are interlinked through corners and edges to form polyanionic slabs running along the direction of the *b* axis. The chains of corner- and edge-shared $CdBi_4$ tetrahedra are further interconnected via sets of *exo*-Bi bonds to form infinite layers propagating along the *a* and *c* axes (Figures 1 and 2). The Ba cations separate these layers by filling the channels and pockets between them. Similar bonding arrangements are known for many E−Tr−Pn compounds (E = alkali, alkaline-earth, or divalent rare-earth metals; Tr = group 13 elements (i.e. triels); Pn = group 15 elements (i.e., pnicogens)).[6−9,12] The structures of some ternary E−T−Pn compounds (T = transition metals with d^0, d^5, or d^{10} configurations) also feature tetrahedrally coordinated transition metals in a wide array of bonding patterns, from isolated TPn_4 blocks to oligomers, chains, layers, and 3D-networks with collapsed channels.[14]

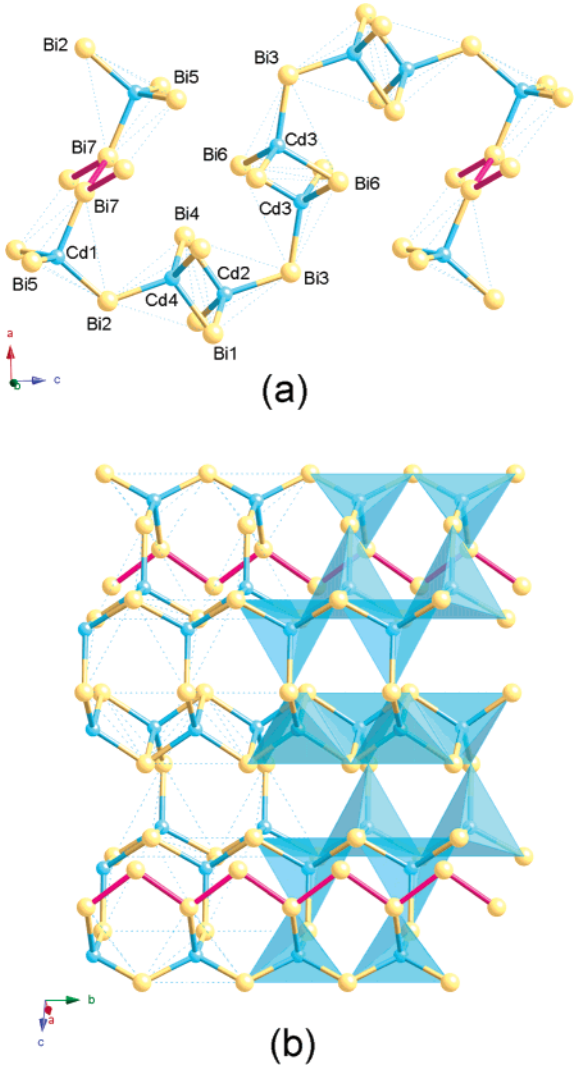

Figure 2. Detailed drawings of the $[Cd_8Bi_{14}]^{22-}$ polyanionic motif in $Ba_{11}Cd_8Bi_{14}$, viewed in parallel (a) and perpendicular (b) to the direction of the layer of propagation. Bond distances are listed in Table 3.

(30) Park, S.-M.; Kim, S.-J. *J. Solid State Chem.* **2004**, *177*, 3418−3422.
(31) (a) Holm, A. P.; Park, S.-M.; Condron, C. L.; Kim, H.; Klavins, P.; Grandjean, F.; Hermann, R. P.; Long G. J.; Kanatzidis, M. G.; Kauzlarich, S. M.; Kim, S.-J. *Inorg. Chem.* **2003**, *42*, 4660−4667. (b) Brown, D. E.; Johnson, C. E.; Grandjean, F.; Hermann, R. P.; Kauzlarich, S. M.; Holm, A. P.; Long, G. J. *Inorg. Chem.* **2004**, *43*, 1229−1234.
(32) Holm, A. P.; Olmstead, M. M.; Kauzlarich, S. M. *Inorg. Chem.* **2003**, *42*, 1973−1981.

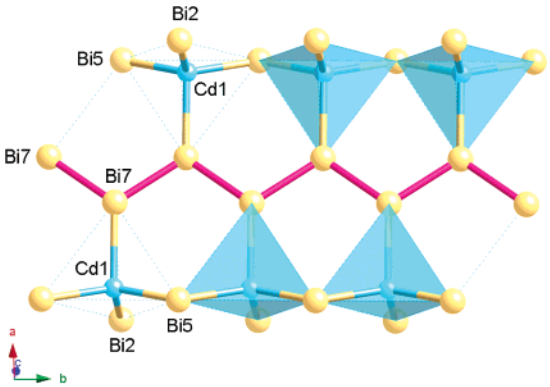

Figure 3. Novel Bi−Bi zigzag chain in $Ba_{11}Cd_8Bi_{14}$.

A closer look at the "wavelike" framework reveals that the recurring segments are basically composed of eight $CdBi_4$ tetrahedra, connected along the *c* direction in the following manner: *corner−edge−corner−edge−corner−edge−corner* (Figure 2). Each repeating unit, in turn, is made up of two crystallographically equivalent $[Cd_4Bi_7]$ quadruplets, which are related by the center of symmetry as shown in Figure 2a. The presence of a 2-fold symmetry along the *b* axis and a mirror plane perpendicular to it results in some "twisting" and "puckering" of the ribbons, which in turn accounts for the relatively large *a* and *c* cell constants. Complex polyanionic networks of similar topology (i.e. variations of corner- and edge-shared tetrahedra) are reported for $BaGa_2Sb_2$,[7] $Sr_{11}Cd_6Sb_{12}$,[30] $Eu_{10}Mn_6Sb_{13}$,[31] $Ba_3Ga_4Sb_5$,[33] and Sr_2MnSb_2,[34] for instance, all of which crystallize in lower-symmetry space groups (monoclinic or orthorhombic) with fairly large unit cell volumes.

Perhaps the most interesting feature of the new structure is in the way the one-dimensional $[Cd_8Bi_{14}]$ slabs are linked to each other via external Bi bonds (Figure 3). These Bi−Bi bonding interactions between terminal bismuth atoms (Bi7 in the present notation) not only bridge the building blocks to form infinite layers but also result in the formation of unique zigzag chains of Bi atoms running parallel to the *b* axis (Figure 1). Such zigzag chains are not known for any other Bi intermetallic compounds; however, structures containing isolated Bi_2 dimers,[35−37] Bi_3 trimers,[38] and Bi_4 tetramers [39] have already been reported. Interestingly, similar infinite Sb−Sb chains are well-known motifs in a variety of antimony-rich compounds,[14] $CaSb_2$,[40] $Ba_4In_8Sb_{16}$,[15] and $Ba_2Sn_3Sb_6$,[9] to name just a few.

The Bi−Bi distances in the chain are 3.055(2) Å and compare well with the Bi−Bi distances in elemental Bi (3.064 Å)[41] or in K_3Bi_2 (Bi_2 dimers with d_{Bi-Bi} = 3.013 Å)[37] and K_5Bi_4 (Bi_4 tetramers with d_{Bi-Bi} = 3.019 Å).[39] These are much shorter than the Bi−Bi contacts in the structures of $Ba_{11}Bi_{10}$ (d_{Bi-Bi} > 3.152 Å),[36] or $Ba_{14}MnBi_{11}$ (d_{Bi-Bi} > 3.335 Å),[38] where some nonclassical motifs such as Bi_4 squares and practically linear Bi_4 tetramers or linear Bi_3 trimers are present, respectively. All of the above, together with the fact that the Bi−Bi−Bi angle is 122.87(5)°, very close indeed to 120° (Figure 3), suggest that all Bi7 atoms are likely to adopt the sp^2 hybridization with significant mixing of the s and p states. Coincidentally, these zigzag motifs are the cause for the small positional disorder described in the Experimental Section. This may suggest that the local symmetry that generates the series of equidistant Bi atoms might be broken as a result of the loose coordination of Bi7. Nonetheless, all attempts to model this disorder in noncentrosymmetric groups failed (see Supporting Information).

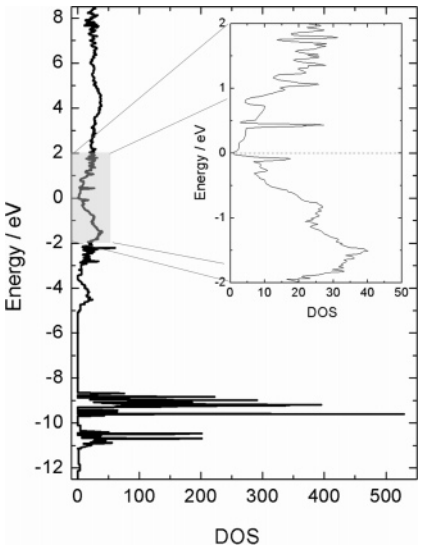

Figure 4. Total DOS for $Ba_{11}Cd_8Bi_{14}$, with inset showing the presence of a small gap at the Fermi level.

All other relevant interatomic distances are listed in Table 3. Bi−Cd, Bi−Ba, and Cd−Ba contacts compare well with those reported for similar binary or ternary intermetallic compounds. In fact, according to the band-structure analysis, the interactions between Ba cations and the polyanionic framework are shown to be relatively unimportant for the overall bonding, unlike in $Ba_5In_4Bi_5$, for example, where the Ba participation in the bonding is substantial.[42] Furthermore, the interactions between the Ba and the Cd atoms are weaker than those between Ba and Bi. This result also supports the closed-shell model for each four-coordinated Cd and implies that the bonding in $Ba_{11}Cd_8Bi_{14}$ can effectively be rationalized using the Zintl formalism.[1−5] According to this concept, the three-bonded bismuths, Bi1, Bi4, Bi6, and Bi7, will have no formal charge (i.e. Bi^0), and the remaining two-bonded bismuths, Bi2, Bi3, and Bi5, would be assigned as Bi^{1-}. All

(33) Park, S.-M.; Kim, S.-J.; Kanatzidis, M. G. *J. Solid State Chem.* **2003**, *175*, 310−315.
(34) Park, S.-M.; Kim, S.-J.; Kanatzidis, M. G. *Inorg. Chem.* **2005**, *44*, 4979−4982.
(35) Xu, L.; Bobev, S.; EI-Bahraoui, J.; Sevov, S. C. *J. Am. Chem. Soc.* **2000**, *122*, 1838−1839.
(36) Derrien, G.; Tillard-Charbonnel, M.; Manteghetti, A.; Monconduit, L.; Belin, K. *J. Solid State Chem.* **2002**, *164*, 169−175.
(37) Gascoin, F.; Sevov, S. C. *J. Am. Chem. Soc.* **2000**, *122*, 10251−10252.
(38) Kuromoto T. Y.; Kauzlarich, S. M.; Webb D. J. *Chem. Mater.* **1992**, *4*, 435−440.
(39) Gascoin, F.; Sevov, S. C. *Inorg. Chem.* **2001**, *40*, 5177−5181.
(40) Deller, K.; Eisenmann, B. *Z. Anorg. Allg. Chem.* **1976**, *425*, 104−108.
(41) Cucka, P.; Barrett, C. S. *Acta Crystallogr.* **1962**, *15*, 865−872.
(42) Ponou S.; Fässler T. F.; Tobias G.; Canadell, E.; Cho, A.; Sevov, S. C. *Chem.−Eur. J.* **2004**, *10*, 3615−3621.

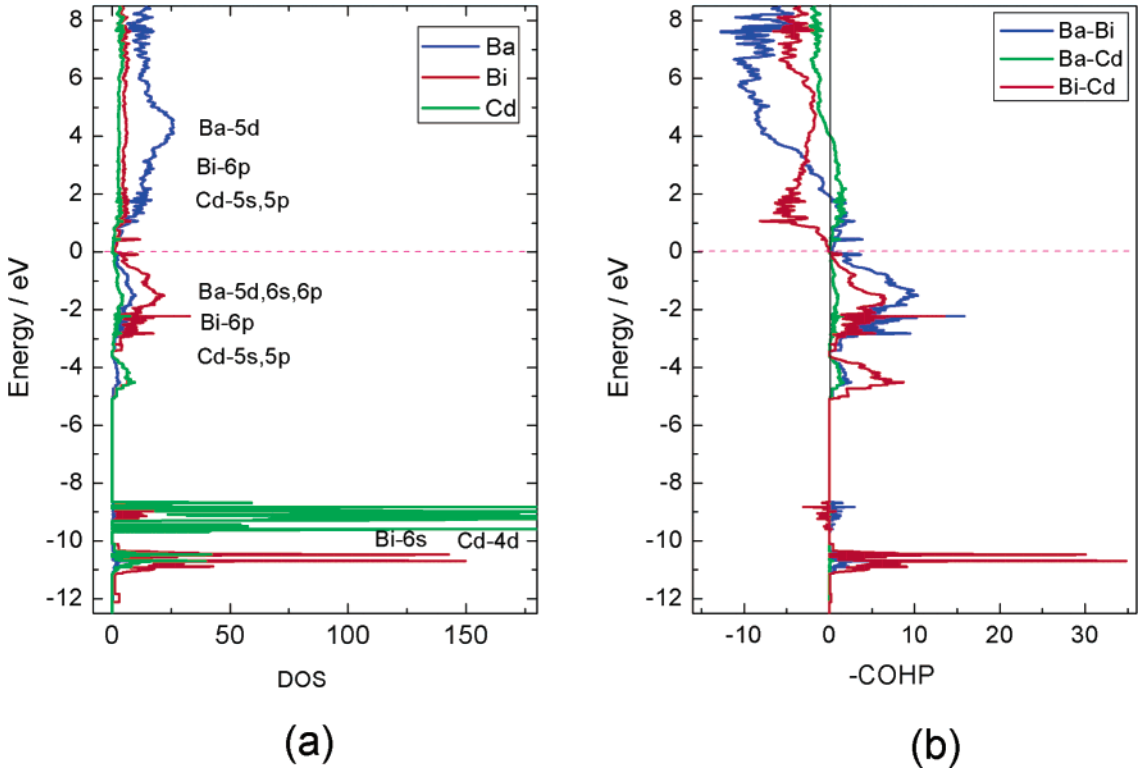

Figure 5. Partial DOS (a) and −COHP (b) for $Ba_{11}Cd_4Bi_{14}$.

Cd atoms are tetrahedrally coordinated and thus can be assigned as Cd^{2-}. Consequently, the compound can be regarded as an electron-precise according to the formulation $(Ba^{2+})_{11}[(Cd^{2-})_8(Bi^{1-})_6(Bi^0)_8]$. Although overly simplistic, this description seems to adequately account for the global bonding picture in $Ba_{11}Cd_8Bi_{14}$ and is supported by the electronic calculations (below).

Electronic Structure. Electronic band structure calculations were performed for the title compound using the TB-LMTO-ASA method. The calculated total DOS is plotted in Figure 4, and it indicates that the Fermi level does not cross any band. Indeed, a very small band gap is present (less than 0.1 eV), which is a consequence of the fact that the filled anion-based and the empty cation-based states are well separated in the energy landscape. Because of the approximations required by this method, the calculated absolute value will be more or less arbitrary.

There are two distinctively different regions in the DOS curve (Figure 5a): a lower region with localized states originated mainly from the 6s states of Bi and the 4d states of Cd and an upper region split by the Fermi level, which is composed of mainly the Ba 5d−6s−6p, Cd 5s−5p, and the Bi 6p bands. Combined with the results shown in the corresponding crystal orbital Hamilton population diagram (Figure 5b), these results lead to several important conclusions: (1) contributions to Bi−Cd bonding interactions near the Fermi level mainly originate from the 5s and 5p states of Cd and the 6p states of Bi, (2) Bi−Cd mixing also predominantly contributes to the nearest band right above the Fermi level, (3) the Ba−Cd interactions are rather weak and could be treated as almost nonbonding, (4) Ba−Bi interactions are stronger than the Ba−Cd interactions and weaker than the Bi−Cd ones, and (5) the Bi−Bi interactions within the zigzag chain are also indicative of strong covalent-type bonding as evidenced from the integrated COHP (the calculated value of 1.223 is much larger than the −iCOHP value of 0.132 for the Bi2−Bi2 pair with d = 3.406(2) Å; this distance compares to the interlayer separations in elemental Bi for instance). More detailed information on the contribution to the overall bonding from different atomic interactions in the form of −iCOHP is tabulated in the Supporting Information.

According to these results, the strong covalent Bi−Cd bonds that are the backbone of the polyanionic framework will be the key factor in governing the structure and the properties of this compound. This supports the above-mentioned Zintl formalism and the closed-shell nature of $Ba_{11}Cd_8Bi_{14}$, which is expected to exhibit narrow-gap semiconducting or rather poor metallic properties.

Conclusions

A new ternary compound, $Ba_{11}Cd_8Bi_{14}$, was synthesized from the corresponding elements using excess Cd to act as a metal flux. It crystallizes with a new monoclinic structure, which can be viewed as layered polyanionic framework composed of unique $[Cd_8Bi_{14}]$ slabs, which are further interconnected through Bi−Bi bonds. Although pnictide−pnictide bonding does not seem to be without precedents, infinite linear or zigzag chains of As, Sb, or Bi are not as common as isolated anions, square nets, or bridging Pn−Pn exo-bonds.[14] Unique bonding patterns exist in the structures

of $BaGa_2Sb_2$,[7] $Ba_3Ga_4Sb_5$,[33] and $Cs_7In_4Bi_6$,[43] for example, which are based on $GaSb_4$ or $InBi_4$ tetrahedra that share corners, edges, or both. In these structures, the building units, however, are connected into 3D polyanionic networks through Ga−Ga or In−In bonds, not by Sb−Sb or Bi−Bi interactions. In that sense, the structure of $Ba_{11}Cd_8Bi_{14}$ presents a new bonding pattern and a new model for connecting slabs, based on Bi_4 tetrahedra, into layers or possibly frameworks via Bi−Bi chains. Electronic band structure calculations showed a very small band gap in the DOS, which implies that this compound could exhibit desirable electronic and possibly thermoelectric properties. Because of the cumbersome synthesis and low yield, coupled with the high sensitivity to air, $Ba_{11}Cd_8Bi_{14}$ is unlikely to find applications as a potential thermoelectric material.

Acknowledgment. S.B. acknowledges financial support from the University of Delaware Research Foundation (UDRF) and from the University of Delaware through a start-up grant.

Supporting Information Available: An X-ray crystallographic file in CIF format, along with detailed analysis on the structure refinements in lower symmetry, plots of the cations' coordination environments, and a table with detailed −iCOHP data. This material is available free of charge via the Internet at http://pubs.acs.org.

IC060583Z

(43) Bobev, S.; Sevov, S. C. *Inorg. Chem.* **1999**, *38*, 2672−2675.